

Size-dependent hot-phonon dynamics in graphene flakes

Benjamin V. Cuning, Kunie Ishioka, Christopher L. Brown, and Dave Kielpinski

Citation: [Applied Physics Letters](#) **104**, 181907 (2014); doi: 10.1063/1.4875580

View online: <http://dx.doi.org/10.1063/1.4875580>

View Table of Contents: <http://scitation.aip.org/content/aip/journal/apl/104/18?ver=pdfcov>

Published by the [AIP Publishing](#)

Articles you may be interested in

[Temperature dependence of the Raman spectra of polycrystalline graphene grown by chemical vapor deposition](#)
Appl. Phys. Lett. **105**, 023108 (2014); 10.1063/1.4890388

[Electronic transport properties of top-gated epitaxial-graphene nanoribbon field-effect transistors on SiC wafers](#)
J. Vac. Sci. Technol. B **32**, 012202 (2014); 10.1116/1.4861379

[Top oxide thickness dependence of remote phonon and charged impurity scattering in top-gated graphene](#)
Appl. Phys. Lett. **102**, 183506 (2013); 10.1063/1.4804432

[Ultrafast dynamics of hot electrons and phonons in chemical vapor deposited graphene](#)
J. Appl. Phys. **113**, 133511 (2013); 10.1063/1.4799377

[Ultrafast relaxation dynamics of hot optical phonons in graphene](#)
Appl. Phys. Lett. **96**, 081917 (2010); 10.1063/1.3291615

The image shows the cover of an Applied Physics Reviews journal issue. It features a blue and orange color scheme with a molecular structure background. The text 'NEW Special Topic Sections' is prominently displayed in white. Below it, 'NOW ONLINE' is written in yellow, followed by the title 'Lithium Niobate Properties and Applications: Reviews of Emerging Trends' in white. The AIP Applied Physics Reviews logo is in the bottom right corner.

NEW Special Topic Sections

NOW ONLINE
Lithium Niobate Properties and Applications:
Reviews of Emerging Trends

AIP Applied Physics
Reviews

Size-dependent hot-phonon dynamics in graphene flakes

Benjamin V. Cuning,^{1,a)} Kunie Ishioka,² Christopher L. Brown,¹ and Dave Kielpinski³

¹Queensland Micro- and Nanotechnology Centre, Griffith University, Brisbane, QLD 4111, Australia

²Nano Characterization Unit, National Institute for Materials Science, Tsukuba 305-0047, Japan

³Centre for Quantum Dynamics, Griffith University, Brisbane, QLD 4111, Australia

(Received 2 March 2014; accepted 27 April 2014; published online 9 May 2014)

We examine the ultrafast carrier phonon dynamics in graphene flakes with different lateral sizes. By using a size-selective centrifugation technique, we create graphene films with graphene flake sizes in the region of 120–450 nm. The transient transmission exhibits two-step relaxation, which are attributed to carrier thermalization followed by hot phonon cooling. We find that the cooling of the hot phonons proceeds faster, by a factor of three, for the smallest graphene flakes. © 2014 AIP Publishing LLC. [<http://dx.doi.org/10.1063/1.4875580>]

Graphene has attracted significant interest in emerging electronic and photonic devices owing to high mobilities, massless charge carriers, and the absence of a band gap.¹ These unique properties have allowed the realisation of a variety of devices such as photodetectors,^{2,3} flexible electronics,⁴ and high-frequency transistors.⁵ Carrier and phonon dynamics play an important role in device limits, for example, in photodetectors, the carrier recombination time affects the total intrinsic response time, with faster recombination resulting in a quicker response rate. In graphene-based electronic devices, the role of heat dissipation in few-monolayer graphene becomes an important issue in device design, as phonon temperatures in graphene-based devices have been demonstrated reaching in excess of 1500 K.^{6–8} Whilst lattice defects are known to hasten carrier recombination in graphene,⁹ the carrier and phonon dynamics of graphene constrained to sub-micron size lateral dimensions still remains poorly understood.

The carrier relaxation dynamics of graphene has been studied extensively by ultrafast pump-probe spectroscopy. These studies have primarily concentrated on epitaxial^{9–15} and exfoliated^{16–19} graphene, although liquid suspensions of graphene flakes have also been studied.²⁰ Theoretical simulations reproduce the main features and timescales of these experiments quite well,^{21–23} indicating that the basic mechanisms of carrier relaxation are well understood. Immediately after optical excitation, the electrons (holes) relax down (up) to the Dirac point and thermalise to a Fermi-Dirac distribution with an effective electronic temperature well over 1000 K but with a much lower lattice temperature. Over the next few hundred femtoseconds, the carriers cool by optical phonon emission and come into equilibrium with the optical phonons. The hot optical phonons themselves decay on the picosecond timescale. During the last process, reabsorption of the hot optical phonons by the carriers keeps the effective carrier temperature high. Hence, the long-time cooling rate of the carriers is set by the cooling rate of the optical phonons, a phenomenon known as the “hot phonon effect.” This picture of the carrier dynamics is also confirmed by saturable absorption,^{20,24,25}

time-resolved Raman spectroscopy,⁷ and time-resolved, angle-resolved photoemission measurements.^{14,15}

The cooling of hot optical phonons has attracted particular attention in these studies, since it is the rate-limiting step for relaxation of optically excited carriers. Early studies have indicated that the cooling rate for optical phonons is dependent on graphene crystallite size and/or basal plane defects as measured by the Raman intensity ratio of the D and G bands, with a higher defect concentration allowing more rapid relaxation.⁹ Additionally, it has been demonstrated that both the carrier cooling¹⁶ and the phonon decay²⁶ proceed more slowly as the number of graphene layers increases. So far, however, there is no data on the effect of flake size on carrier dynamics.

Here, we show that the lateral size of graphene flakes substantially affects the hot-phonon relaxation time. We obtain pump-probe data on flake-graphene films containing different lateral sizes of flakes, and find that the picosecond decay of transient reflectivity depends strongly on flake size. Our data indicate that the anharmonic decay of optical phonons into acoustic phonons is accelerated by as much a factor of three as the flake size is reduced from ≈ 445 nm down to ≈ 120 nm.

To prepare samples of graphene flakes with different sizes, we employ the graphene synthesis methodology pioneered by the group of Coleman. This synthetic technique utilises the effect of sonication on flake graphite in water-surfactant solution to separate the flake graphite into few-layer graphene in solution.²⁷ Subsequent centrifugation at varying speeds allows solution samples of distinct lateral sizes to be isolated.²⁸ In our work, the centrifuge accelerations undergone by our samples, 3000 g, 10 000 g, and 16 000 g, are much larger than those previously reported, allowing for much smaller lateral sizes. (We report accelerations, rather than rotation speeds, to ease comparison with results in the literature that use centrifuge rotors of different radii.) Subsequent slow vacuum filtration and substrate transfer allows thin films of mostly flat-laying graphene to be examined.^{29–31}

A typical image of the edge of such a film obtained by scanning electron microscopy and isolated using a centrifuge acceleration of 10 000 g is shown in Figure 1. As we show later, such accelerations yield an average flake size of

^{a)}Author to whom correspondence should be addressed. Electronic mail: b.cuning@griffith.edu.au.

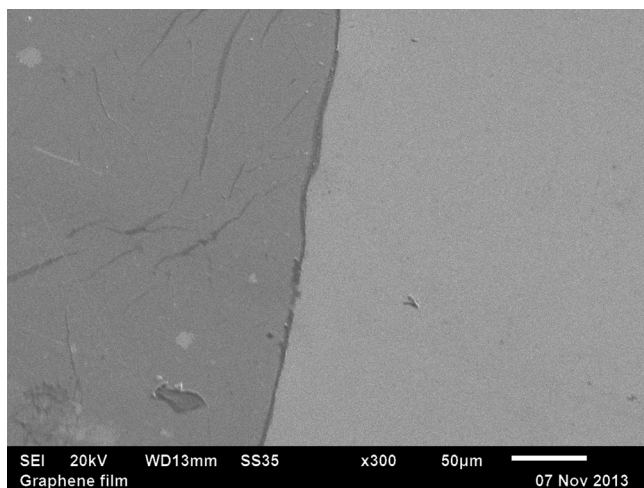


FIG. 1. Scanning electron micrograph of a typical centrifuged flake-graphene film. The edge of the film can be seen as the vertical line bisecting the image.

185 nm with 2–3 atomic layers per flake. The optical absorption was measured to be 61% at 800 nm, so from the well-known single-layer absorption of 2.3%,³² we infer that the film thickness in Figure 1 contains approximately 40 graphene atomic layers (i.e., 13–20 flakes). Films like these are highly porous and contain substantial amounts of residual surfactant^{29,30} which increase the total film thickness (graphene flakes, residual surfactant, and empty space) to much more than 40 atomic layers.

Flake sizes are estimated based on the hydrodynamic size as measured by dynamic light scattering (DLS) (Figure 2). As shown by Lotya *et al.*, there is a reliable empirical relationship (Eq. (1)) between the graphene flake hydrodynamic size d_{DLS} as measured by DLS and the actual size d_0 as measured by transmission electron microscopy³³

$$d_{DLS} = \alpha d_0^\beta, \quad (1)$$

where $\alpha = 5.9 \pm 2.2$ and $\beta = 0.66 \pm 0.06$. The relative flake sizes are also estimated by Raman spectroscopy (Figure 3) due to the increase in D/G ratio with decreasing lateral size.

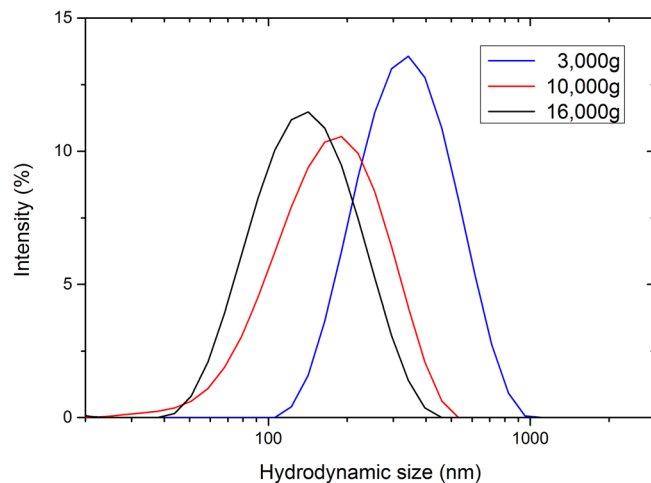


FIG. 2. DLS hydrodynamic size plot of the centrifuged graphene samples. These data correspond to a graphene flake lateral size of 445 nm (3000 g), 185 nm (10 000 g), and 120 nm (16 000 g).

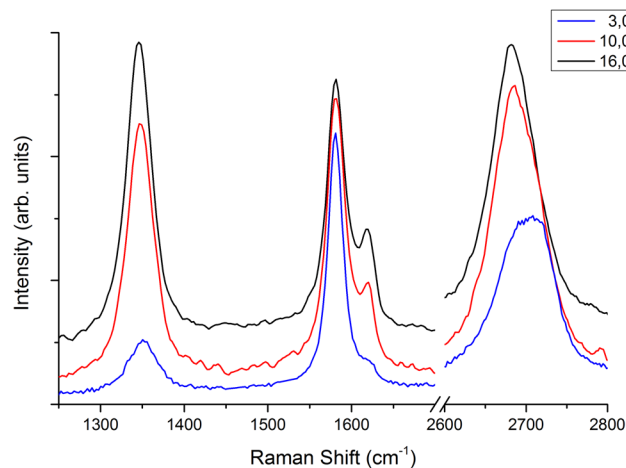


FIG. 3. Raman spectra of graphene samples prepared at centrifuge accelerations of 16 000 g (black), 10 000 g (red), and 3 000 g (blue) covering the D, G, and 2D bands. Spectra are normalized by the G band intensity and offset for clarity.

As Raman excitation within ≈ 50 nm of a graphene edge gives rise to a prominent D band, even in monocrystalline graphene,³⁴ the higher “edge concentration” of smaller flakes under the focused Raman spot size allows us to confirm that higher centrifugation speeds result in smaller flake dimensions. The narrow linewidth of the G band confirms our graphene films contain few basal plane defects. Hence, the D/G ratio can be regarded as measuring the fraction of the flake area that lie close to an edge, or to put it more simply, the flake size.

To perform pump-probe measurements, we transfer films of flake graphene onto glass microscope slides. For each centrifuge speed (3000, 10 000, and 16 000 g), we test several films of different thicknesses, ranging from 17% to 73% linear absorption at 800 nm wavelength. Transient transmission measurements are performed at room temperature under ambient conditions. The fundamental output from a Ti:sapphire oscillator with 10 fs duration, 800 nm centre wavelength, and 80 MHz repetition rate is used to excite and monitor carriers near the K point of graphene. Linearly polarized pump and probe beams are focused onto the same spot on the sample surface with a diameter of $\sim 30 \mu\text{m}$. The probe beam is monitored before and after transmission through the sample with a pair of matched photodiodes, and their signals are subtracted in order to minimize the noise due to the laser intensity fluctuations. The pump-induced change in the transmission ΔT is measured with a lock-in technique, while the time delay between the pump and probe pulses is scanned with a computer-controlled translational stage. This technique enables us to observe transmission changes as small as $\Delta T/T < 10^{-6}$.

Examples of our pump-probe results for films of large and small flakes are shown in Figure 4. Following an initial sharp dip, we observe an overshoot to positive $\Delta T/T$ with a time constant of 100–200 fs, followed by its recovery to zero on a subpicosecond to picosecond timescale. Based on the previous studies,^{14,18,23} we ascribe the fast transient to equilibrium between the photoexcited carriers and the optical phonons, and the slow transient to the cooling of the hot optical phonons. We fit the time traces to a double-exponential

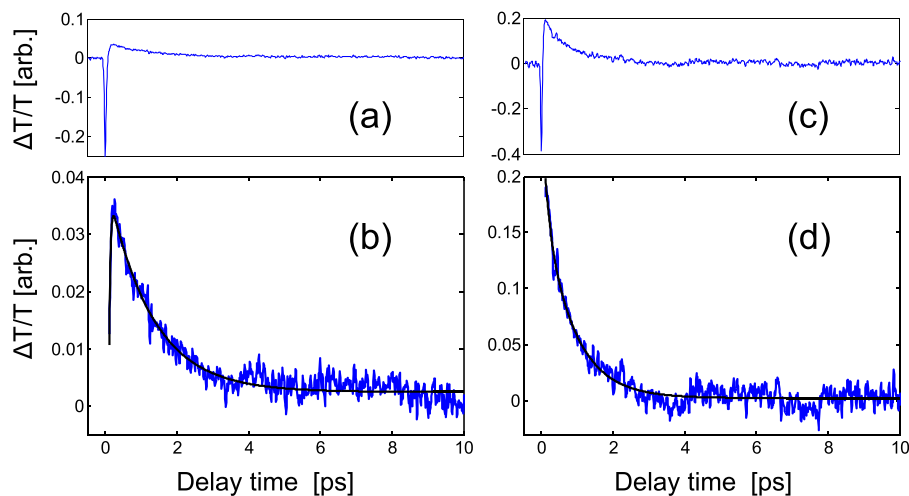


FIG. 4. Pump-probe transient transmission of flake graphene: (a) and (b) samples with centrifuge acceleration of 3000 g and total film absorption of 55%, (c) and (d) samples with centrifuge acceleration of 16000 g and total film absorption of 33%. Blue lines in (b) and (d) show magnified versions of the slow transients in (a) and (c). Black curves in (b) and (d) represent an exponential fitting to the experimental data.

function to obtain the time constants τ_1 and τ_2 of the fast and slow relaxation processes. We did not observe a significant size dependence for τ_1 . However, τ_2 depends strongly on the flake size, as is clear by comparing the left and right panels of Figure 4.

We study the cooling dynamics of the optical phonons as a function of flake size by quantitatively analysing the time constant of the slow transient. To this end, we fit a sum of two exponential functions to our data and extract the two time constants τ_1 and τ_2 of the fast and slow transients. With a naïve fitting procedure, noise in the fast transient can easily obscure the beginning of the much weaker slow transient, yielding unreliable results for τ_2 . We avoid these problems by fitting only the portion of the data taken after a minimum 150 fs delay. The fitted time constants are found to be independent with respect to variations of the minimum delay around the chosen value of 150 fs, indicating that this fitting procedure accurately represents the true time constants.

The time constant τ_2 obtained from an exponential fitting of the transmission traces after 150 fs is shown for the full range of samples in Figure 5. There is a clear trend

towards shorter time constants for the higher centrifuge accelerations, indicating that the optical phonons cool faster. On the other hand, the time constant of the slow transient does not appear to be systematically correlated with the total optical absorption. We therefore present the average values of the time constants for each centrifugation speed (right of Figure 5), to clearly indicate the extent of the trend. Higher centrifugation speeds result in smaller flakes that also have fewer atomic layers. In principle, the change in phonon cooling rate could arise either from the change in flake size or from the change in the number of layers per flake. However, pump-probe measurements on large, exfoliated graphene multilayers have shown that increasing the number of layers from 1 to 11 increases the slow time constant only slightly, from 2.5 to 3.2 ps.¹⁶ The effect seen here is much stronger—a threefold decrease in time constant—and most of our measurements show time constants far smaller than 2.5 ps.

The data in Figure 5 indicate that the change in cooling rate is associated with the flake size, rather than the substrate coupling effect previously seen in experiments with epitaxial graphene¹² or some other effect associated with film thickness. The films with low optical absorption are thinner, so a larger fraction of the flakes in the low-absorption samples reside close to the surface. Hence, a substrate coupling effect would lead to faster cooling for low-absorption samples. Such a trend is not evident in the data, so substrate coupling appears to play a minor role in our experiment. This conclusion is reasonable in light of the film morphology, as the flakes are very weakly coupled to the substrate as compared to epitaxial graphene. The flake-graphene film is highly porous and, though the individual flakes lie more or less parallel to the substrate, the stacking of the flakes is random.^{29,30} The contact between flakes, or between the flakes and the substrate, is minimal.

Although our data do not allow us to determine the cause of the increased cooling rate, we can speculate about possible mechanisms. In large, pristine graphene sheets without excited carriers, optical phonon cooling proceeds by two processes: (1) anharmonic decay of an optical phonon into two acoustic phonons and (2) decay of a phonon into a low-energy electron-hole pair.^{23,35,36} However, electron-hole pair creation is not an effective phonon cooling mechanism in ultrafast pump-probe experiments, since the carriers remain

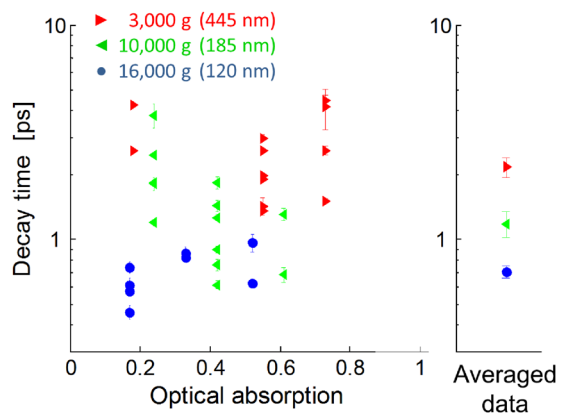


FIG. 5. Fitted time constants of the slow transient of centrifuged flake-graphene samples. Left: Results of individual measurements taken at various positions on the samples. A systematic trend to shorter decay time can be seen at higher centrifugation speed (smaller flake size). There is no clear dependence on the optical absorption of the samples. Error bars are the statistical uncertainties in the fits. Right: Average decay rates for the three centrifugation speeds. Error bars are the standard error computed from all data at a given flake size.

in thermal equilibrium with the optical phonons. The obvious remaining possibility is that scattering from the flake edge promotes anharmonic decay. We are unaware of any theoretical studies of anharmonic phonon scattering at the edges of 2-D structures, so this is an open question. It is also possible that the anharmonic coupling constant is simply larger for small flakes, even away from the edge. Recent calculations of the mechanical properties of graphene flakes indicate that a large buckling stress of the whole flake sets in for small flakes. This stress induces changes in the elastic constants on the order of 10% for flakes smaller than 50 nm,³⁷ so significant effects might still be expected for our flake sizes.

In conclusion, we have synthesised graphene films consisting of small lateral size graphene through a size-selective centrifugation technique, generating flakes of ≈ 120 –450 nm lateral size. By measuring the reflectivity recovery time after a high fluence optical pulse using pump-probe spectroscopy, we have found the reflectivity of smaller flakes equilibrate over a much shorter time scale, suggesting the optical phonons in laterally constrained graphene flakes cool significantly faster. Graphene-substrate and graphene-graphene interactions are excluded as a possible cause, while no new cooling mechanisms appear present. The apparent speedup of the existing cooling mechanisms is a tantalizing topic for future theoretical inquiry.

D.K. was supported by an Australian Research Council Future Fellowship (FT110100513).

- ¹K. S. Novoselov, V. I. Falko, L. Colombo, P. R. Gellert, M. G. Schwab, and K. Kim, *Nature* **490**, 192 (2012).
- ²X. Gan, R.-J. Shiue, Y. Gao, I. Meric, T. F. Heinz, K. Shepard, J. Hone, S. Assefa, and D. Englund, *Nat. Photonics* **7**, 883 (2013).
- ³T. Mueller, F. Xia, and P. Avouris, *Nat. Photonics* **4**, 297 (2010).
- ⁴T.-H. Han, Y. Lee, M.-R. Choi, S.-H. Woo, S.-H. Bae, B. H. Hong, J.-H. Ahn, and T.-W. Lee, *Nat. Photonics* **6**, 105 (2012).
- ⁵Y. Wu, Y.-m. Lin, A. A. Bol, K. A. Jenkins, F. Xia, D. B. Farmer, Y. Zhu, and P. Avouris, *Nature* **472**, 74 (2011).
- ⁶D.-H. Chae, B. Krauss, K. von Klitzing, and J. H. Smet, *Nano Lett.* **10**, 466 (2010).
- ⁷S. Wu, W.-T. Liu, X. Liang, P. J. Schuck, F. Wang, Y. R. Shen, and M. Salmeron, *Nano Lett.* **12**, 5495 (2012).
- ⁸S. Berciaud, M. Y. Han, K. F. Mak, L. E. Brus, P. Kim, and T. F. Heinz, *Phys. Rev. Lett.* **104**, 227401 (2010).
- ⁹J. M. Dawlaty, S. Shivaraman, M. Chandrashekar, F. Rana, and M. G. Spencer, *Appl. Phys. Lett.* **92**, 042116 (2008).
- ¹⁰D. Sun, Z.-K. Wu, C. Divin, X. Li, C. Berger, W. A. de Heer, P. N. First, and T. B. Norris, *Phys. Rev. Lett.* **101**, 157402 (2008).

- ¹¹H. Wang, J. H. Strait, P. A. George, S. Shivaraman, V. B. Shields, M. Chandrashekar, J. Hwang, F. Rana, M. G. Spencer, C. S. Ruiz-Vargas, and J. Park, *Appl. Phys. Lett.* **96**, 081917 (2010).
- ¹²L. Huang, G. V. Hartland, L.-Q. Chu, Luxmi, R. M. Feenstra, C. Lian, K. Tahy, and H. Xing, *Nano Lett.* **10**, 1308 (2010).
- ¹³K. M. Dani, J. Lee, R. Sharma, A. D. Mohite, C. M. Galande, P. M. Ajayan, A. M. Dattelbaum, H. Htoon, A. J. Taylor, and R. P. Prasankumar, *Phys. Rev. B* **86**, 125403 (2012).
- ¹⁴J. C. Johannsen, S. Ulstrup, F. Cilento, A. Crepaldi, M. Zacchigna, C. Cacho, I. C. E. Turcu, E. Springate, F. Fromm, C. Raidel, T. Seyller, F. Parmigiani, M. Grioni, and P. Hofmann, *Phys. Rev. Lett.* **111**, 027403 (2013).
- ¹⁵I. Gierz, J. C. Petersen, M. Mitrano, C. Cacho, I. C. E. Turcu, E. Springate, A. Stöhr, A. Köhler, U. Starke, and A. Cavalleri, *Nature Mater.* **12**, 1119 (2013).
- ¹⁶R. W. Newson, J. Dean, B. Schmidt, and H. M. van Driel, *Opt. Express* **17**, 2326 (2009).
- ¹⁷M. Breusing, S. Kuehn, T. Winzer, E. Malić, F. Milde, N. Severin, J. P. Rabe, C. Ropers, A. Knorr, and T. Elsaesser, *Phys. Rev. B* **83**, 153410 (2011).
- ¹⁸P. J. Hale, S. M. Hornett, J. Moger, D. W. Horsell, and E. Hendry, *Phys. Rev. B* **83**, 121404 (2011).
- ¹⁹M. M. Leandro, M. Kin Fai, A. H. C. Neto, N. M. R. Peres, and F. H. Tony, *New J. Phys.* **15**, 015009 (2013).
- ²⁰S. Kumar, M. Anija, N. Kamaraju, K. S. Vasu, K. S. Subrahmanyam, A. K. Sood, and C. N. R. Rao, *Appl. Phys. Lett.* **95**, 191911 (2009).
- ²¹S. Butscher, F. Milde, M. Hirtschulz, E. Malić, and A. Knorr, *Appl. Phys. Lett.* **91**, 203103 (2007).
- ²²E. Malić, T. Winzer, E. Bobkin, and A. Knorr, *Phys. Rev. B* **84**, 205406 (2011).
- ²³B. Y. Sun, Y. Zhou, and M. W. Wu, *Phys. Rev. B* **85**, 125413 (2012).
- ²⁴G. Xing, H. Guo, X. Zhang, T. C. Sum, and C. H. A. Huan, *Opt. Express* **18**, 4564 (2010).
- ²⁵Z. Zhang and P. L. Voss, *Opt. Lett.* **36**, 4569 (2011).
- ²⁶K. Sho, K. Ikufumi, A. Shunsuke, F. Hirokazu, S. Maki, K. Masahiro, and T. Jun, *Appl. Phys. Express* **4**, 045101 (2011).
- ²⁷J. S. Ronan, L. Mustafa, and N. C. Jonathan, *New J. Phys.* **12**, 125008 (2010).
- ²⁸U. Khan, A. O'Neill, H. Porwal, P. May, K. Nawaz, and J. N. Coleman, *Carbon* **50**, 470 (2012).
- ²⁹S. De, P. J. King, M. Lotya, A. O'Neill, E. M. Doherty, Y. Hernandez, G. S. Duesberg, and J. N. Coleman, *Small* **6**, 458 (2010).
- ³⁰M. Lotya, P. J. King, U. Khan, S. De, and J. N. Coleman, *ACS Nano* **4**, 3155 (2010).
- ³¹B. V. Cunning, C. L. Brown, and D. Kiepiniski, *Appl. Phys. Lett.* **99**, 261109 (2011).
- ³²R. R. Nair, P. Blake, A. N. Grigorenko, K. S. Novoselov, T. J. Booth, T. Stauber, N. M. R. Peres, and A. K. Geim, *Science* **320**, 1308 (2008).
- ³³L. Mustafa, R. Aliaksandra, F. D. John, and N. C. Jonathan, *Nanotechnology* **24**, 265703 (2013).
- ³⁴A. K. Gupta, T. J. Russin, H. R. Gutiérrez, and P. C. Eklund, *ACS Nano* **3**, 45 (2009).
- ³⁵N. Bonini, M. Lazzeri, N. Marzari, and F. Mauri, *Phys. Rev. Lett.* **99**, 176802 (2007).
- ³⁶J. Lin, L. Guo, Q. Huang, Y. Jia, K. Li, X. Lai, and X. Chen, *Phys. Rev. B* **83**, 125430 (2011).
- ³⁷S. Bera, A. Arnold, F. Evers, R. Narayanan, and P. Wölfle, *Phys. Rev. B* **82**, 195445 (2010).